Combinatorial characterization of cell interactions with polymer surfaces

J. Carson Meredith,[1,5] Joe-L. Sormana,[1] Benjamin G. Keselowsky,[2] Andrés J. García,[2,3] Alessandro Tona,[4] Alamgir Karim,[5] Eric J. Amis[5]

[1]School of Chemical Engineering, Georgia Institute of Technology, 311 Ferst Dr., Atlanta, Georgia 30332-0100

[2]Georgia Tech/Emory Department of Biomedical Engineering, Georgia Institute of Technology, 315 Ferst Dr., Atlanta, Georgia 30332-0360

[3]Woodruff School of Mechanical Engineering, Georgia Institute of Technology, 801 Ferst Dr., Atlanta, Georgia 30332-0405

[4]Biotechnology Division, National Institute of Standards and Technology, 100 Bureau Dr., Gaithersburg, Maryland 20899-8310

[5]Polymers Division, National Institute of Standards and Technology, 100 Bureau Dr., Gaithersburg, Maryland 20899-8540

Abstract: We report a novel combinatorial methodology for characterizing the effects of polymer surface features on cell function. Libraries containing hundreds to thousands of distinct chemistries, microstructures, and roughnesses are prepared using composition spread and temperature gradient techniques. The method enables orders of magnitude increases in discovery rate, decreases variance, and allows for the first time high-throughput assays of cell response to physical and chemical surface features. The technique overcomes complex variable spaces that limit development of biomaterial surfaces for control of cell function. This report demonstrates these advantages by investigating the sensitivity of osteoblasts to the chemistry, microstructure, and roughness of poly(D,L-lactide) and poly(ε-caprolactone) blends. In particular, we use the phenomenon of heat-induced phase separation in these polymer mixtures to generate libraries with diverse surface features, followed by culture of UMR-106 and MC3T3-E1 osteoblasts on the libraries. Surface features produced at a specific composition and process temperature range were discovered to enhance dramatically alkaline phosphatase expression in both cell lines, not previously observed for osteoblasts on polymer blends. © 2003 Wiley Periodicals, Inc. J Biomed Mater Res 66A: 483–490, 2003

Key words: combinatorial; osteoblasts; polymer; tissue engineering; surface interactions

INTRODUCTION

Perhaps the most vital need for developing polymeric biomaterials is surfaces that actively control cellular and physiologic responses. Such "bioactive" polymers could be used in tissue engineering scaffolds that support and regulate the adhesion, growth, and function of target cells. Signaling in natural tissues occurs through binding of soluble and extracellular matrix (ECM) biomolecules, as well as *nonspecific* ECM physical and chemical features. ECM is a multicomponent mixture assembled into well-defined microstructures with characteristic chemistry and roughness. Most signaling research has focused on discovering specific chemical pathways that regulate cell function. However, a growing literature indicates that surface structural features dramatically affect cell function, shape, cytoskeletal tension, and regulatory pathways.[1–11] Extensive investigation with capillary endothelial cells, for example, has shown that distortion in cell shape changes the sensitivity to signaling molecules and alters the gene program and cell fate.[2,12–15] It has also been suggested that nuclear shape, which may be influenced by the overall cell shape and cytoskeletal tension, can affect gene expression and protein synthesis.[16] Superior bioactive materials can be designed only by taking into consideration *both* the well-studied signaling chemistry and the often-neglected *physical and nonspecific chemical surface features.*
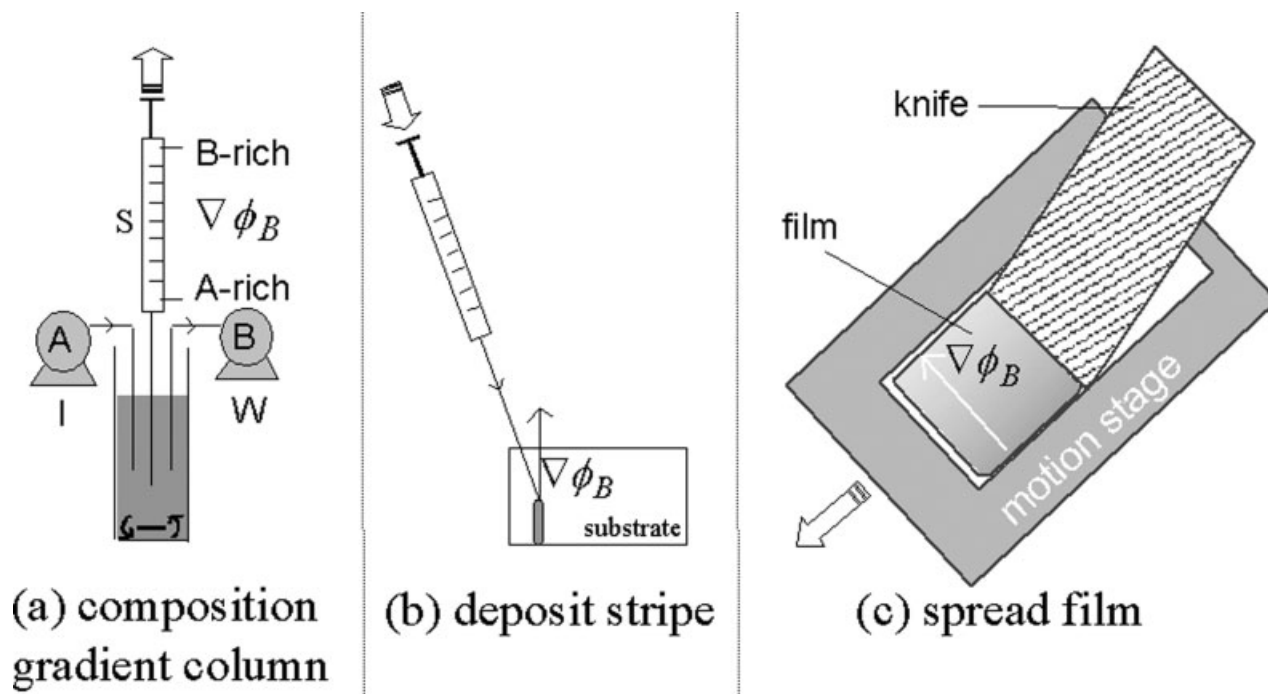
Figure 1. Schematic of the continuous composition gradient deposition process.

The challenge to achieving a better understanding of surface effects stems from the large variable space (composition and processing conditions) and complex phenomena that control material surface features. These complexities overwhelm conventional one-sample for one-measurement approaches to biomaterials evaluation. This challenge has been addressed in signaling chemistry, gene expression, and in biomaterials synthesis with the development of high-throughput and combinatorial experimental strategies.[17,18] These include plate readers, DNA microarrays, and electrophoretic-chromatographic gradient libraries. Unfortunately, combinatorial methods for investigating the effects of *surface features* on cell function are *not available*. Such an innovation would speed discovery and improve the quality of hypothesis testing and materials development by assaying cell response to large numbers of surface features in a single experiment. To address this challenge, we developed a novel strategy for preparing *gradient* combinatorial polymer surface libraries with property gradients that cover thousands of compositions, annealing temperatures, and surface structures. These methods have been demonstrated in characterizing numerous polymer surface structuring phenomena.[19]

In this article, we apply the gradient-library methods to assay the effect of biodegradable polymer surface features and chemistry on osteoblast cell function. One advantage is that biomaterial candidates failing to elicit desired biological responses are rejected quickly, so that detailed characterization is focused on the most promising materials. The method also accelerates fundamental characterization of bioactive polymers by

allowing rapid correlations among polymer composition, processing, surface properties, and cell response. Specifically, we investigate the use of surface features in blends of poly(D,L-lactide) (PDLA) and poly(ε-caprolactone) (PCL) to control cell function. These polymers are FDA-approved for use in certain devices, and their blends exhibit lower critical solution temperature (LCST) phase behavior,[20] resulting in phase-separation upon heating to create diverse microstructures and roughnesses.

MATERIALS AND METHODS

Preparation of composition gradient libraries

PDLA ($M_w = 127{,}000$,[21] $M_w/M_n = 1.56$, Alkermes) and PCL ($M_w = 114{,}000$, $M_w/M_n = 1.43$, Aldrich) were obtained from commercial suppliers.[22] Each T-ϕ combinatorial library consists of a polymer film on a clean silicon (Si-H/Si) wafer, with dimensions of 25×30 mm along orthogonal gradients in ϕ_{PCL} and annealing T. The composition gradient deposition process, shown in Figure 1, is applicable to a wide range of polymer blends and is described in detail elsewhere.[23] Briefly, a PCL solution in CHCl$_3$ is pumped into a mixing vial initially containing a PDLA solution while the mixture is withdrawn, resulting in a linear increase in PCL composition in the vial. A third automated syringe extracts the ϕ-gradient solution from the vial and deposits it as a thin stripe on the substrate. A knife-edge coater spreads the liquid as a film orthogonal to the composition gradient. FTIR spectroscopy was used to measure compositions to within mass fraction 4% on libraries by obtaining spectra in the C—H stretch regime (2700 to 3100) cm^{-1}.

Temperature gradient annealing

To explore a large processing T range, the ϕ-gradient films were annealed on a T-gradient heating stage, with the T-gradient *orthogonal* to the ϕ-gradient. This custom aluminum T-gradient stage[23] uses a heat source and a heat sink to produce a linear gradient ranging between adjustable end-point temperatures. We verified that the relatively weak composition (3 mass %/mm) and temperature (1.5°C/mm) gradients do not induce appreciable flow or diffusion over the experimental time scale.[23]

Cell culture

After annealing T-ϕ libraries for 2 h to generate diverse phase-separated structures, the libraries were *quenched to room temperature* and placed in multiwell culture plates. Two cell lines were used to alleviate concerns that observations of enhanced proliferation and function were artifacts of the cell line. UMR-106 (ATCC, Manassas, VA) and MC3T3-E1 (Riken Cell Bank, Tokyo, Japan) osteoblasts were cultured separately on the libraries for periods of 4 h, 1 day, and 5 days in α-modified Eagle's medium supplemented with 10% fetal bovine serum, 100 μg/mL streptomycin, 100 μg/mL penicillin, and 0.25 μg/mL amphotericin B at 37°C and 5% CO_2. The MC3T3-E1, from fetal mouse bones, and UMR-106, established from a transplantable rat osteosarcoma, are clonal cell lines that have been studied extensively and exhibit expression products characteristic of differentiated osteoblasts.[24–27] These markers include osteocalcin, alkaline phosphatase, osteopontin, matrix Gla protein, mineralization, and activity regulation by parathyroid hormone and 1,25-dihydroxyvitamin D_3, among others. Cells were seeded at 10,000 cells/cm^2 (5-day series) and 5000 cells/cm^2 (1-day series). At termination, cultures were washed three times with 1 mL of phosphate-buffered saline (PBS), and were fixed in volume fraction 3% formaldehyde in PBS at 4°C for 5 min (UMR-106) or in mass fraction 70% ethanol/30% water for 45 min at room temperature (MC3T3-E1). Cells were cultured at identical conditions on tissue culture polystyrene (TCPS) coverslips as a uniform surface control.

Cell density and morphology were assayed by optical and fluorescence microscopy, taking a 10×10 grid of 100 images over each cultured library. For qualitative identification of cell density and morphology, cultures were treated with Safranin for general optical identification, or with the fluorescent dyes bis-benzimide trihydrochloride for DNA and rhodamine-conjugated phalloidin for F-actin identification. Retention of osteoblast-like phenotype was assessed qualitatively by staining for alkaline phosphatase with Sigma kit 86-C (UMR-106) and with a histochemical procedure based upon Na-α-napthyl phosphate and fast blue RR salt (MC3T3-E1).[28] The UMR-106 and MC3T3-E1 cultures were performed in separate laboratories at NIST and Georgia Tech, respectively, and different sterilization, fixation, and staining procedures were used in each lab, which helps to establish the generality of the methods.

RESULTS AND DISCUSSION

Figure 2(A) shows the linear variation in PCL composition on a ϕ-gradient library from FTIR spectroscopy, along with AFM and optical microscope images indicating the diverse microstructures formed on a T-ϕ gradient library as a result of PCL/PDLA phase separation and PCL crystallization. Each library explores a wide range in processing T $(75 < T < 135)$°C, and composition $(0 < \phi_{PCL} < 0.8)$. The phase-separated microstructures have sizes from ≈0.2 μm to ≈300 μm, a range extending from well below to far above the size of osteoblasts. At low ϕ_{PCL} values, AFM [Fig. 2(B)] indicates an amorphous PDLA-rich matrix containing dispersed semicrystalline PCL-rich regimes with diameters of (0.23 ± 0.07) μm, for $\phi_{PCL} = 0.10$, and (0.34 ± 0.08) μm, for $\phi_{PCL} = 0.20$, independent of temperature. Larger PCL regions with both semicontinuous and droplet morphologies are observed as ϕ_{PCL} and T are raised into the LCST phase-separation region, consistent with spinodal decomposition and nucleation-growth mechanisms of phase separation. At T, ϕ_{PCL} values below the LCST boundary, semicrystalline PCL is uniformly dispersed within an amorphous PDLA-rich matrix.

Osteoblasts cultured directly on the libraries (post-annealing) indicate that cell adhesion and function are influenced strongly by these surface microstructures. Figure 3 shows digital photographs of T-ϕ libraries stained with Safranin [Fig. 3(A)] and for alkaline phosphatase [Fig. 3(B)] following a 5-day culture with UMR-106. The white curve is a guide to the eye for the LCST cloud point boundary, and indicates phase-separated (inside LCST curve) and homogeneous (outside LCST curve) regions. UMR-106 adhere to some extent over the entire T, ϕ range, but adhesion and proliferation occur preferentially at regions within the LCST two-phase regime. Figure 3(B) indicates qualitatively that alkaline phosphatase is detected for cells attached at all T and ϕ, but alkaline phosphatase expression is enhanced significantly within the LCST regime. In contrast to the T-ϕ libraries, Figure 3(C) shows a uniform TCPS control surface with uniform cell coverage and alkaline phosphatase expression.

Figure 3(D) and (E) presents digital photographs of 5-day MC3T3-E1 library cultures stained for alkaline phosphatase. The darkest stained elliptical regions near the LCST phase boundary (right center of library) show a strong enhancement in alkaline phosphatase expression relative to the rest of the library and the TCPS control. The region of enhanced alkaline phosphatase corresponds to processing conditions of $(96°C < T < 110)$°C and $0.4 < \phi_{PCL} < 0.55$. This regime of enhanced alkaline phosphatase expression might be missed entirely or misinterpreted as aberrant data if T and ϕ were screened with a small number of individual samples, as is the conventional practice.
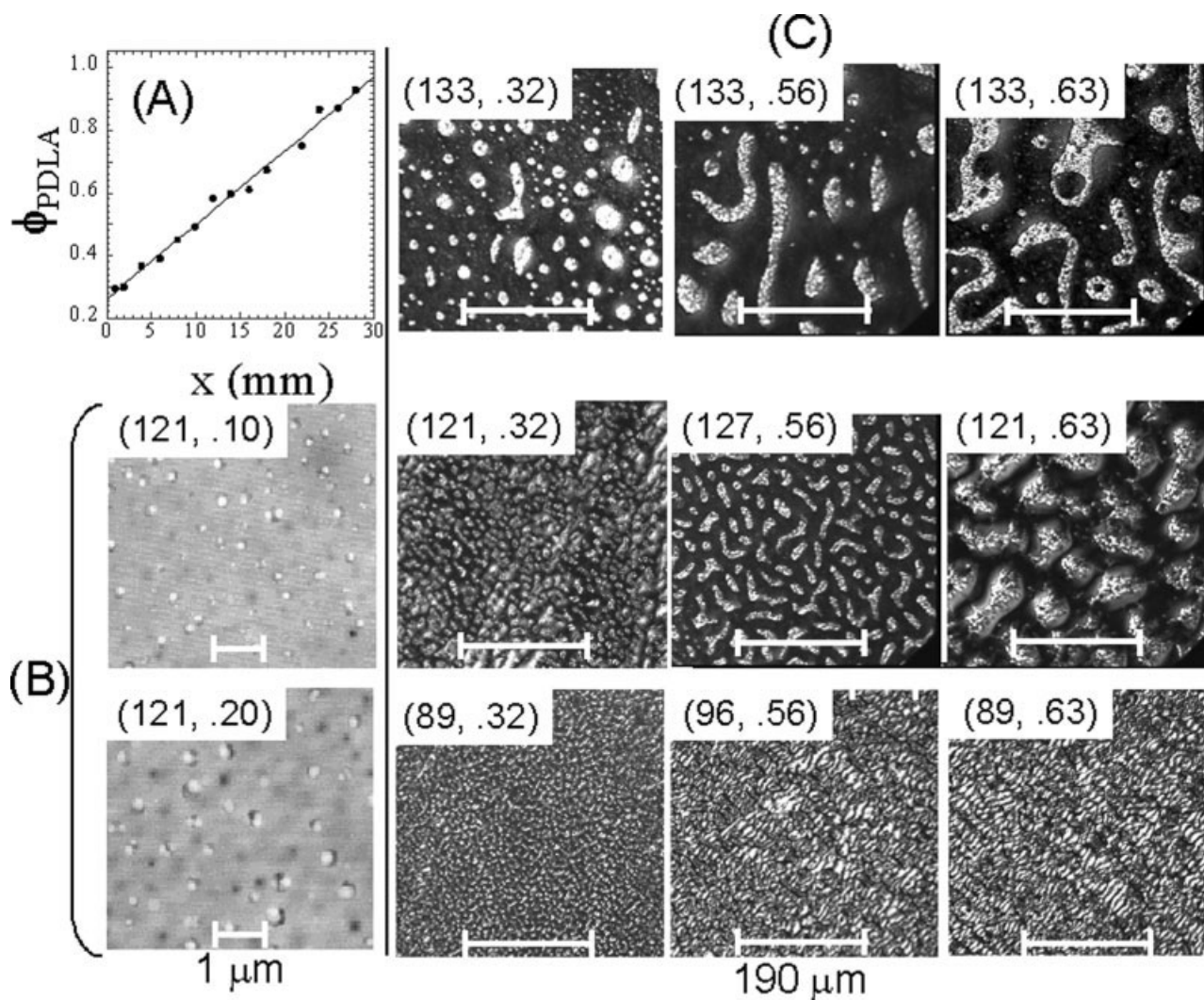
Figure 2. (A) Composition (mass fraction) of PDLA measured with FTIR spectroscopy on a continuous film ϕ-gradient PDLA/PCL library. (B) AFM and (C) crossed-polar optical micrographs of selected regions from a PDLA/PCL T-ϕ library illustrating the diverse morphologies generated with LCST-type phase separation. The scale bar in (C) is 190 μm and the numbers in parentheses are (T, ϕ_{PCL}). The PCL-rich regimes are identified as the droplet phase in the AFM images and bright regions in optical images. All images were taken from the same T-ϕ library at room temperature, post annealing.

However, the gradient library provides a facile approach for direct observation of such trends. In particular, a previously unknown surface microstructure, optimized for osteoblast function, has been observed on blends of these common biomaterials proposed for orthopaedic tissue engineering applications.[29]

Cells presented a spread and multipolar morphology at most T, ϕ_{PCL} values, as seen in images of confluent UMR-106 cells (from within the LCST regime) in Figure 4(A), nonconfluent cells (outside the LCST regime) in Figure 4(B), and MC3T3-E1 in Figure 4(E) and (F). UMR-106 cultured on some regimes outside the LCST regime were rounded [Fig. 4(C)], and the cell surface coverage, a measure of adhesion and proliferation, approaches confluency only at T, ϕ_{PCL} values within and close to the LCST two-phase regime. Interestingly, UMR-106 cells were not confluent at $T > 120°C$, deep within the LCST regime, suggest-

ing a maximum amount of tolerable surface phase separation. These trends for UMR-106 are in good agreement with control cultures performed on uniform PDLA/PCL blend surfaces at $\phi_{PCL} = 0.2$, 0.36, and 0.5. These uniform surface cultures also showed a dramatic decrease in the density of adhered cells above $\phi_{PCL} = 0.5$. In contrast, the MC3T3-E1 were confluent over the entire T, ϕ_{PCL} library, but preferentially expressed alkaline phosphatase only in a small region of T, ϕ_{PCL} processing conditions.

Cell proliferation and alkaline phosphatase expression are enhanced on the heterogeneous surfaces within the LCST phase-separated region relative to the more homogeneous surface regions and TCPS controls. The primary surface differences between regions within and outside the LCST are the microstructure (lateral distribution of chemically distinct domains) and surface roughness. AFM and optical images from
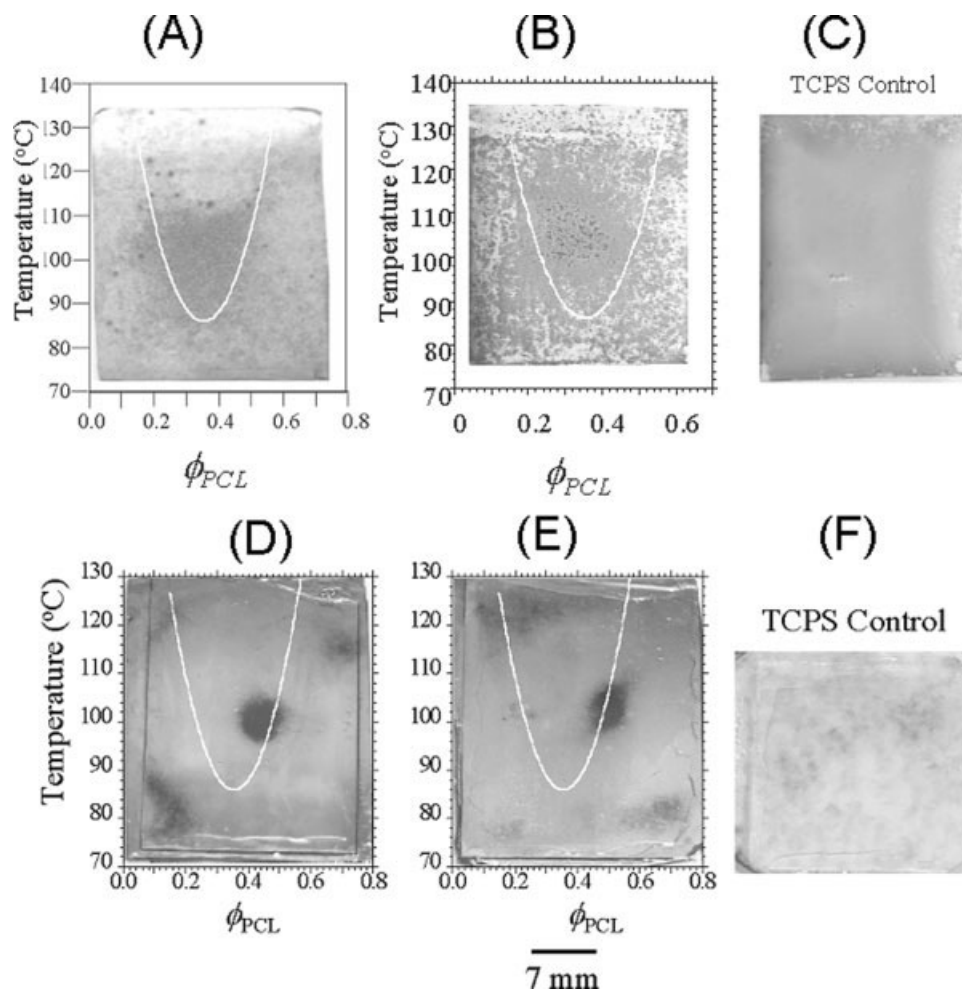
Figure 3. (A) Safranin stained and (B) alkaline phosphatase stained T-ϕ libraries after 5-day culture with UMR-106 cells, showing preferential adhesion and alkaline phosphatase expression on T-ϕ regions approximately within the PDLA/PCL two-phase LCST regime. (C) Alkaline phosphatase stained tissue culture polystyrene control slide after 5 days; cultured with UMR-106 cells concurrently with the libraries. (D, E) Alkaline phosphatase stained T-ϕ libraries after 5-day culture with MC3T3-E1 cells. (F) Alkaline phosphatase stained TCPS control slide for (D, E).

libraries were used to quantify the surface roughness and microstructure sizes. The diameter of PCL-rich regimes, d_{PCL}, increases with both ϕ_{PCL} and T (Fig. 5), and covers a range of $(0.2 < d_{PCL} < 60)$ μm. Beyond $d_{PCL} = 60$ μm the PCL phase becomes continuous with dispersed PDLA droplets. The fraction of surface area occupied by PCL-rich regimes, $\phi_{PCL,S}$ (Fig. 6), increases with ϕ_{PCL} but *decreases* with T over the range $(0.01 < \phi_{PCL,S} < 0.9)$. As T is increased above the LCST boundary at constant ϕ_{PCL}, the rate of growth of phase-separated microstructures increases and PCL-rich regimes consolidate in order to lower interfacial area. The result is a decrease in PCL-rich surface area at higher T. Phase separation also induces changes in the roughness of the surface, attributed to surface tension differences between chemically distinct domains and between crystalline and amorphous PCL. With a few exceptions root-mean-square (rms) surface roughness, R, increases with both ϕ_{PCL} and T over a range of $(2 < R < 500)$ nm (Fig. 7).

Literature evidence has shown that surface nonspe-cific chemistry, microstructure, and roughness influ-ence cell adhesion, proliferation, and differentia-tion.[2,4–11,30] These surface features may influence focal adhesion formation that subsequently determines cell shape and cytoskeletal tension. Changes in cell geom-etry induced by physical and mechanical ECM fea-tures can cause cells cultured *in vitro* to switch be-tween gene programs, independent of the chemical signaling environment.[2,12–15,31] For microstructure, capillary endothelial cells cultured on microfabricated islands spread and proliferated on the largest islands, rounded, and underwent apoptosis on the smallest islands, and differentiated to form hollow capillary tubes on the medium-sized islands.[14] For roughness, previous studies observe that osteoblasts and other cells adhere and proliferate preferentially on rough-ened surfaces,[4–9,30] although much of this work in-volves metal surfaces. For example, mesenchymal cells form focal attachments that span the space be-tween surface peaks on roughened Ti surfaces,[32] al-lowing optimal spreading only for certain peak
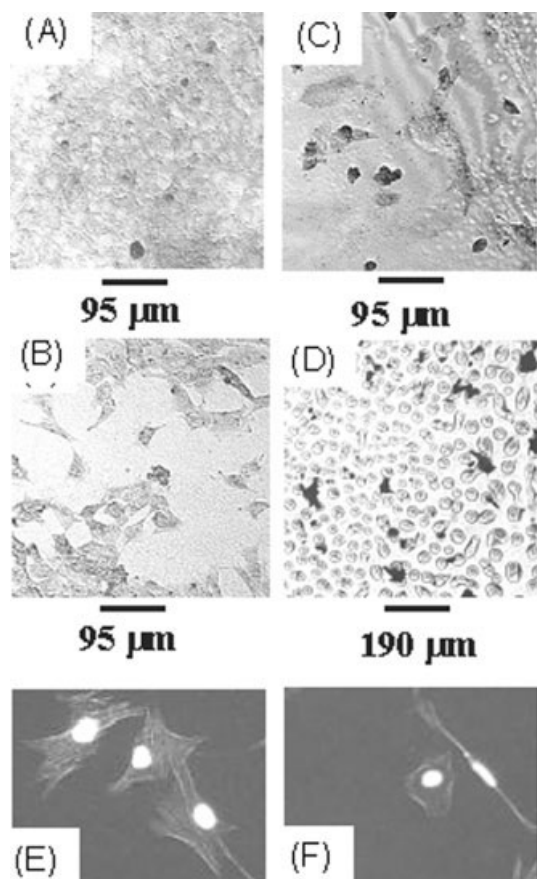
Figure 4. Optical micrographs of UMR-106 from various regions on libraries. (A) Confluent, spread cells within the LCST regime, $T = 111°C$, $\phi_{PCL} = 0.44$, 5-day culture. (B) Nonconfluent, spread cells outside the LCST regime, $T = 75°C$, $\phi_{PCL} = 0.65$, 5-day culture. (C) Nonconfluent, rounded cells outside the LCST regime, $T = 75°C$, $\phi_{PCL} = 0.24$, 5-day culture. (D) Early culture of UMR-106 that indicates a preferential attachment to PDLA-rich regimes, T 120°C, $\phi_{PCL} = 0.48$, 1-day culture. (E) MC3T3-E1 cells stained for F-actin and DNA from a 4-h culture at $T = 100°C$, $\phi_{PCL} = 0.45$. (F) Same as (E) except $T = 100°C$, $\phi_{PCL} = 0.55$.

heights and spacings. It has also been shown that the relative degree of hepatocyte cell–cell versus cell–polymer interaction can be controlled by adjusting the roughness of PLGA surfaces.[3] Although the precise mechanisms by which cell shape is influenced by surface structures and is translated into selection of biochemical signals are unknown, it is possible that the transduction pathway is closely related to cytoskeletal tension.[2] For example, microcompartments for protein synthesis have been shown to form at focal adhesion points following tension-driven restructuring of the endothelial cell cytoskeleton.[33] In addition, the nuclear shape has been shown to play a role in cell function.[16]

With this interpretation, the chemistry, shape, and size of phase-separated regimes in our system may induce cell shapes and mechanical stresses that lead to enhanced proliferation and upregulation of alkaline phosphatase expression. Phase-separated microstructures present chemically distinct surface regimes to
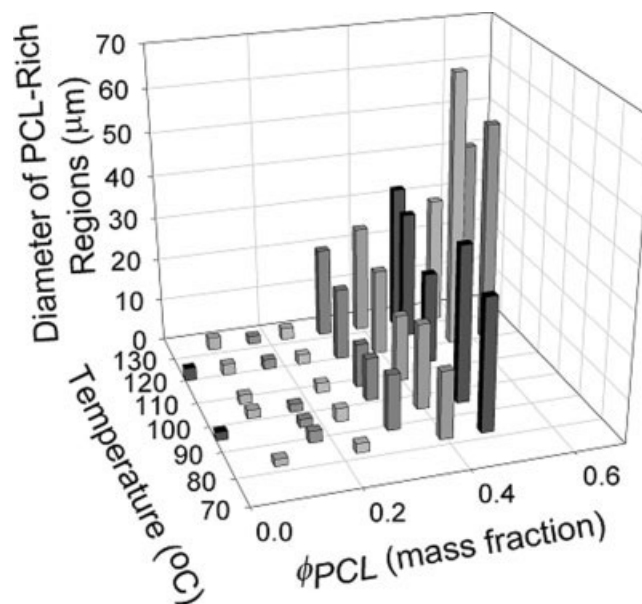

Figure 5. Average effective diameter of PCL-rich regions, d_{PCL}, (μm). The variance in this quantity is ±5%.

cells and optical images indicate that cells appear to attach preferentially on the more hydrophilic PDLA-rich regimes [Fig. 4(D)].[34] The crystalline nature of PCL may also influence this preferential adhesion, as fibroblasts have also been shown to be sensitive to small crystallinity differences on poly(L-lactide).[35] In addition, other workers have observed minimal to no attachment of osteoblast-like stromal bone marrow cells to pure PCL and PCL-rich blends with poly(lactide-co-glycolide).[1] Because the available PDLA-rich surface area changes with T and ϕ_{PCL}, (Figs. 2 and 5),
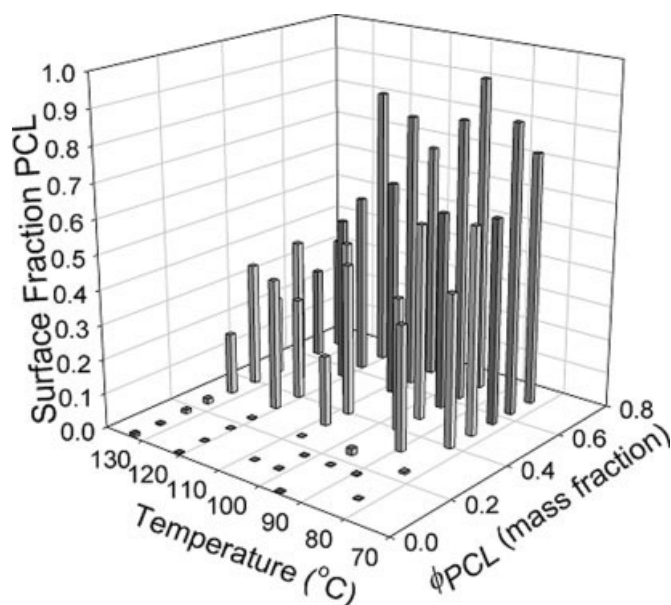

Figure 6. Surface fraction of PCL-rich regimes, $\phi_{PCL,S}$. The variance in this quantity is ±2%.
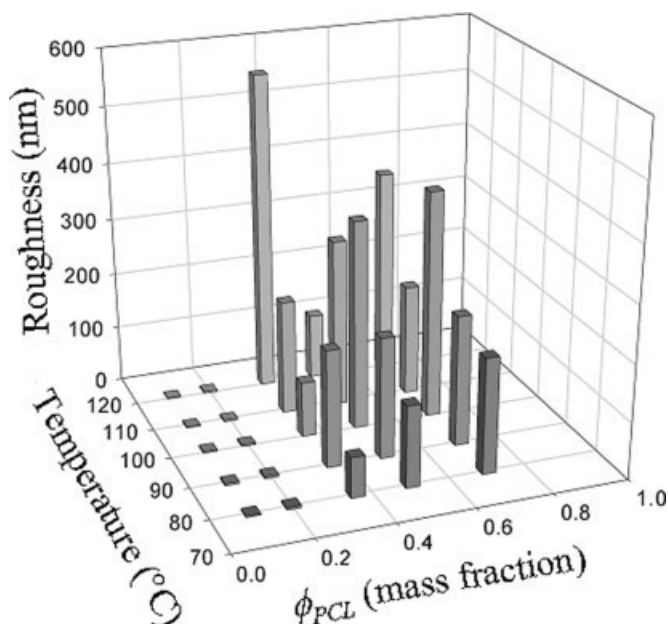
Figure 7. Root-mean-square surface roughness, R (nm). The variance in this quantity is $\pm 5\%$.

cells are forced to adopt different shapes to maximize contact with PDLA.

For example, Figure 4(E) and 4(F) show fluorescence images taken from MC3T3-E1 libraries stained for DNA (Hoechst) and F-actin (rhodamine phalloidin) after 4-h culture. The cells demonstrate enhanced F-actin production and multipolar spreading [Fig. 4(E)] within the regime of enhanced alkaline phosphatase expression, $T = 100°C$, $\phi_{PCL} = 0.45$. In contrast, cells cultured on surfaces just outside of the enhanced alkaline phosphatase regime, at $T = 100°C$, $\phi_{PCL} = 0.55$, show significantly less F-actin, poorer spreading, and an axial morphology [Fig. 4(F)]. Microstructure sizes within the preferential alkaline phosphatase expression regime may promote cell spreading across distances sufficient to induce stresses that enhance F-actin production, which correlates with the enhanced alkaline phosphatase expression in Figure 3(D) and (E). The T-ϕ libraries allow rapid identification of the preferred microstructural feature sizes: these are ($2 < d_{PCL} < 37$) μm for UMR-106 and ($30 < d_{PCL} < 40$) μm for MC3T3-E1. Hence, the UMR-106 cells showed enhanced AlP expression over a wider range of microstructural sizes than the MC3T3-E1 cells. The surface feature heights where UMR-106 confluency occurs in the present study are (0.63 ± 0.24) μm, with a roughness range of $R = (0.26 \pm 0.16)$ μm. For MC3T3-E1, alkaline phosphatase expression is optimized at a roughness of $R = (0.37 \pm 0.05)$ μm.

At a constant T, the equilibrium *composition* of the PCL-rich and PDLA-rich regimes is *constant* within the LCST regime. Hence, only the size and distribution of PCL-rich droplets varies with composition. Thus, at 100°C in Figure 3(D) and (E), the *only* differences be-

tween the surface at $\phi_{PCL} = 0.45$ (enhanced alkaline phosphatase) and $\phi_{PCL} < 0.45$ (nonenhanced alkaline phosphatase) are the surface microstructure and roughness. This observation highlights the important role of surface physical features, particularly lateral and height distribution of chemically distinct domains, even when the surface chemistry of each remains constant.

Serum proteins in culture medium adsorb and coat surfaces before cells begin to attach. Hence, the effects of surface features observed above may be mediated by differences in the amount, conformation, and biologic activity of serum proteins adsorbed, which can also depend on chemical microstructure and roughness.[9] For example, the conformation and biologic activity of fibronectin was found to be adjustable by changing substrate chemistry, which in turn, altered the binding of integrins and proliferation and differentiation of C2C12 myoblasts.[36] Future experiments using these combinatorial methods will involve the design of combinatorial libraries to separate the effects of microstructure, roughness, chemistry, and serum protein adsorption on cell responses to biomaterials. In addition, paracrine signaling between cells cannot be ruled out as a significant factor in the observations reported here. Future combinatorial approaches should also involve control experiments in which intercellular signaling is selectively inhibited, to judge the importance of these effects relative to the surface chemistry and structure.

CONCLUSIONS

The combinatorial library high-throughput technique for varying polymer surface structures allows rapid, efficient, and accurate investigation of the effects of microstructure, roughness, and surface chemistry on cell adhesion and proliferation. The high-throughput physical pattern assay serves as a natural compliment to combinatorial chemistry already in use in pharmaceutical, biomaterials, and genomics research. In particular, the method is ideal for rapid identification of surface features that promote (or reduce) cell adhesion and function, early in the development and characterization of new biomaterials. The surprising result is that from two well-known, FDA-approved materials we have discovered a previously unknown optimal processing temperature and mixture composition that increases dramatically the expression of alkaline phosphatase. We anticipate the applicability of this new method to the characterization of a wide range of complex biomedical polymer–cell systems and its combination with more sophisticated cell proliferation, function, and gene expression assays.

References

1. Calvert JW, Marra KG, Cook L, Kumta PN, DiMilla PA, Weiss LE. Characterization of osteoblast-like behavior of clutured bone marrow stromal cells on various polymer surfaces. J Biomed Mater Res 2000;52:279–284.

2. Huang S, Ingber DE. Shape-dependent control of cell growth, differentiation, and apoptosis: Switching between attractors in cell regulatory networks. Exp Cell Res 2000;261:91–103.

3. Ranucci CS, Moghe PV. Polymer substrate topography actively regulates the multicellular organization and liver-specific functions of cultured hepatocytes. Tissue Eng 1999;5:407–420.

4. Schwartz Z, Martin JY, Dean DD, Simpson J, Cochran DK, Boyan BD. Effect of titanium surface roughness on chondrocyte proliferation, matrix reporduction, and differentiation depends on the state of cell maturation. J Biomed Mater Red 1996;30:145.

5. Wojciak-Stothard B, Madeeja B, Korohoda W, Curtis A, Wilkinson C. Activation of macrophage-like cells by multiple grooved substrata. Topographical controll of cell behaviour. Cell Biol Int 1995;19:485.

6. Von Recum AF, Shannon CE, Cannon CE, Long KJ, Can Kooten TG, Meyle J. Surface roughness, porosity, and texture as modifiers of cellular adhesion. Tissue Eng 1996;2:241.

7. Meyle J, Wolfburg H, Von Recum AF. Surface micromorphology and cellular interactions. J Biomater Appl 1993;7:362.

8. Lampin M, Warocquier-Clerout R, Legris C, Degrange M, Sigot-Luizard MF. Correlation between substratum roughness and wettability, cell adhesion, and cell migration. J Biomed Mater Red 1997;36:99.

9. Boyan BD, Batzer R, Kieswetter K, Liu Y, Cochran DL, Szmuckler-Moncler S, Dean DD, Schwartz Z. Titanium surface roughness alters responsiveness of MG63 osteoblast-like cells to 1 alpha,25-(OH)2D3. J Biomed Mater Res 1998;39:77–85.

10. Wieland M, Chehroudi B, Textor M, Brunette DM. Use of Ti-coated replicas to investigate the effects on fibroblast shape of surfaces with varying roughnes and constant chemical composition. J Biomed Mater Res 2002;60:434–444.

11. Glass-Brudzinski J, Perizzolo D, Brunette DM. Effects of substratum surface topography on the organization of cells and collagen fibers in collagen gel cultures. J Biomed Mater Res 2002;61:608–618.

12. Dike LE, Chen CS, Mrksich M, Tien J, Whitesides GM, Ingber DE. Geometric control of switching between growth, apoptosis, and differentiation during angiogenesis using micropatterned substrates. In Vitro Cell Dev Biol Anim 1999;35:441–448.

13. Folkman J, Moscona A. Role of cell shape in growth control. Nature 1978;273:345–349.

14. Huang S, Chen SC, Ingber DE. Cell-shape-dependent control of p27Kip and cell cycle progression in human capillary endothelial cells. Mol Biol Cell 1998;9:3179–3193.

15. Chen CS, Mrksich M, Huang S, Whitesides GM, Ingber DE. Geometric control of cell life and death. Science 1997;276:1425–1428.

16. Thomas CH, Collier JH, Sfeir CS, Healy KE. Engineering gene expression and protein synthesis by modulation of nuclear shape. Proc Natl Acad Sci USA 2002;99:1972–1977.

17. Chicurel M. Faster, better, cheaper genotyping. Nature 2001; 412:580–582.

18. Brocchini S, James K, Tangpasuthadol V, Kohn J. Structure–property correlations in a combinatorial library of degradable biomaterials. J Biomed Mater Res 1998;42:66–75.

19. Meredith JC, Smith AP, Karim A, Amis EJ. Combinatorial materials science: Thin-film dewetting. Macromolecules 2000; 33:9747–9756.

20. Meredith JC, Amis EJ. LCST phase separation in biodegradable polymer blends: poly(D,L-lactide) and poly(ϵ-caprolactone). Macromol Chem Phys 2000;200:733–739.

21. According to ISO 31-8, the term "molecular weight" has been replaced by "relative molecular mass," M_r. The number average molecular mass is given by M_n.

22. Certain equipment and instruments or materials are identified in the article to adequately specify the experimental details. Such identification does not imply recommendation by the National Institute of Standards and Technology, nor does it imply the materials are necessarily the best available for the purpose.

23. Meredith JC, Karim A, Amis EJ. High-throughput measurement of polymer blend phase behavior. Macromolecules 2000; 33:5760–5762.

24. Gruber R, Nothehegger G, Ho GM, Willhelm M, Peterlik M. Differential stimulation by PGE_2 and calcemic hormones of IL-6 in stromal/osteoblastic cells. Biochem Biophys Res Commun 2000;270:1080–1085.

25. van Leeuwen JPTM, Birkenhager JC, van den Bemd GCM, Pols HAP. Evidence for coordinated regulation of osteoblast function by 1,25-duhydroxyvitamin D_3 and parathyroid hormone. Biochim Biophys Acta 1996;1312:55–62.

26. Partridge NC, Alcorn D, Michelangeli VP, Kemp BE, Ryan GB, J. MT. Functional properties of hormonally responsive cultured normal and malignant rat osteoblastic cells. Endocrinology 1981;108:213–219.

27. Sodek J, Berkman FA. Bone Cell Cultures. Methods Enzymol 1987;145:303–324.

28. McGee-Russel SM. Histochemical methods for calcium. J Histochem Cytochem 1958;6:22–42.

29. Tams J, Joziasse CAP, Bos RRM, Rozema FR, Drijpma DW, Pennings AJ. High-impact poly(L/D-lactide) for grafture fixation: In vitro degradation and animal pilot study. Biomaterials 1995;16:1409–1416.

30. Batzer R, Liu Y, Cochran DL, Szmuckler-Moncler S, Dean DD, Boyan BD, Schwartz Z. Prostaglandins mediate the effects of titanium surface roughness on MG63 osteoblast-like cells and alter cell responsiveness to 1alpha,25-(OH)2D3. J Biomed Mater Res 1998;32:489–496.

31. Singhvi R, Kumar A, Lopez GP, Stephanopoulos GN, Wang DI, Whitesides GM, Ingber DE. Engineering cell shape and function. Science 1994;264:696–698.

32. Groessner-Schreiber B, Tuan RS. Enhanced extracellular matrix production and mineralization by osteoblasts cultured on titanium surfaces in vitro. J Cell Sci 1992;1:209–217.

33. Chicurel ME, Singer RH, Meyer CJ, OIngber DE. Integrin binding and mechanical tension induce movement of mRNA and ribosomes to focal adhesions. Nature 1998;392:730–733.

34. The contact angle of deionized water was measured to be 59° for pure PDLA and 63° for PCL.

35. Park A, Griffith Cima L. In vitro cell response to differences in poly-L-lactide crystallinity. J Biomed Mater Res 1996;31:117–130.

36. García AJ, Vega MD, Boettiger D. Modulation of cell proliferation and differentiation through substrate-dependent changes in fibronectin conformation. Mol Biol Cell 1999;10:785–798.